J Appl Electrochem (2007) 37:1055–1061
DOI 10.1007/s10800-007-9354-9

ORIGINAL PAPER

# Effect of synthesis routes on the performance of hydrated Mn(IV) oxide-exfoliated graphite composites for electrochemical capacitors

**Chuanyun Wan · Kazuhisa Azumi · Hidetaka Konno**

Received: 3 January 2007 / Revised: 15 June 2007 / Accepted: 19 June 2007 / Published online: 10 July 2007


**Abstract** $MnO_2 \cdot nH_2O$-EG composites for electrochemical capacitors were prepared using commercially available low cost exfoliated graphite (EG) as a conductive substrate, and (a) potassium permanganate and (b) manganese(II) acetate solutions by two different routes. Method (1) was addition of EG to (a), followed by 1 h stirring and then slow addition of (b), and in Method (2) the solutions (a) and (b) were swapped. Using Method (1) submicron or smaller sized $MnO_2 \cdot nH_2O$ particles having mesopores were formed, whereas Method (2) produced lumps of aggregated particles of several tens microns without mesopores, though specific surface areas were not very different and both were similar by XRD. Although EG alone showed only about 2 F $g^{-1}$, the capacitance per net amount of $MnO_2$ in 1 mol $L^{-1}$ $Na_2SO_4$ solution increased proportionally with EG content and was always larger by Method (1) than Method (2), that is, the utilization ratio of $MnO_2$ increased with EG content and the effect was more prominent in the case of Method (1). The results indicated that EG is a good conductive material for $MnO_2 \cdot nH_2O$ electrochemical capacitors if appropriate synthesis processes are used. The performance of the composites strongly depends on synthesis method, even using the same raw materials. It was suggested that the morphology of the products was a primary factor leading to different performance rather than composition.

C. Wan (✉)
Department of Chemical Engineering, Shanghai Institute of Technology, Shanghai 200235, P. R. China
e-mail: cywan@citiz.net

K. Azumi · H. Konno
Laboratory of Advanced Materials Chemistry, Graduate School of Engineering, Hokkaido University, Sapporo 060-8628, Japan

**Keywords** Composite · Electrochemical capacitor · Exfoliated graphite · Hydrated Mn(IV) oxide · Synthesis route

## 1 Introduction

Electrochemical capacitors (ECs) are gaining much interest as energy storage devices due to the higher power density and longer cycle life than batteries and the higher energy density than conventional electric double layer capacitors (EDLCs). Hydrated ruthenium oxide has been proved to be an excellent material with remarkable high specific capacitance [1]. However, the high cost of the raw material has prevented this material from commercial application [2]. As a result, several transition metal oxides as cheaper candidates have been studied in recent years. Among them hydrated or amorphous Mn(IV) oxide, $MnO_2 \cdot nH_2O$, has been paid much attention [3–18] because of its low cost, abundance and less harmful nature. Since this material has poor electrical conductivity, different measures have been devised to use it as electrodes, such as either deposition on metals [4, 14, 16, 18], graphite [6, 9, 11, 15] and ITO [8] as thin films, or addition of carbon black [5, 12, 13, 15], acetylene black [3, 7, 10] and carbon nanotubes [16–18] as conductive materials. So far reported specific capacitance with thin film systems is generally higher than that by addition of conductive materials, but the thin film system seems to have a disadvantage from the viewpoint of energy density.

We have reported that exfoliated graphite (EG) is a promising conductive material for $MnO_2 \cdot nH_2O$ [19] and mentioned briefly that the synthesis rout affects the performance of $MnO_2 \cdot nH_2O$ as an electrochemical capacitor. There are many methods to synthesize $MnO_2 \cdot nH_2O$,

including anodic deposition [6, 8, 9, 11, 14, 15, 18], and the reduction of permanganate by Mn(II) species [3–5, 10, 16, 17], reducing agents [7, 12], or thermally [13], based on the formation of colloidal $MnO_2$ [20]. In the present work, the most commonly used method, the reduction of potassium permanganate, $KMnO_4$, by manganese(II) acetate, $Mn(OCOCH_3)_2$, was selected and two different synthesis routes were adopted. The effect of synthesis routes on the electrochemical performance of composites was examined by X-ray diffraction, thermo-gravimetry, nitrogen adsorption/desorption at 77 K, cyclic voltammetry and galvanostatic charge/discharge measurements.

## 2 Experimental

Exfoliated graphite (EG) was commercially available and was of 130 μm nominal diameter. $MnO_2 \cdot nH_2O$-EG composites were synthesized from EG and the stoichiometric amounts of $KMnO_4$ and Mn(II) acetate, by two different routes as follows:

Method (1): Addition of predetermined amounts of EG to 0.1 mol $L^{-1}$ $KMnO_4$ solution → 1 h stirring at ambient temperature → slow addition of 0.15 mol $L^{-1}$ Mn(II) acetate solution → 5 h stirring at ambient temperature.

Method (2): Addition of predetermined amounts of EG to 0.15 mol $L^{-1}$ Mn(II) acetate solution → 1 h stirring at ambient temperature → slow addition of 0.1 mol $L^{-1}$ $KMnO_4$ solution → 5 h stirring at ambient temperature.

Final products were filtered, washed with distilled water and dried at 110 °C for 24 h in air.

X-ray diffraction (XRD; Rigaku, RINT-Ultima+/PC, Cu Kα), observation by scanning electron microscopy (SEM; JEOL, JSM-6300F, 5 kV), nitrogen adsorption/desorption (BEL Japan, BELSORP-mini, 77 K), and thermogravimetric analysis (TG; Seiko Instruments, TG/DTA6300, 10 K $min^{-1}$ in oxygen) were carried out. TG data were used to determine the amount of water, EG, and Mn in the products, as reported previously [19].

10 mass% of poly(tetrafluoroethylene) (PTFE) were added as a binder to the $MnO_2 \cdot nH_2O$-EG composite and working electrodes of electrochemical capacitor were fabricated in the usual way [19]. The amount of composite on the electrode was approximately 10 mg $cm^{-2}$. All electrochemical measurements were carried out in a glass cell with two platinum foil counter electrodes and a saturated calomel electrode (SCE) as reference. Deaerated 1 mol $L^{-1}$ $Na_2SO_4$ solution was used without pH adjustment at room temperature. The capacitance was estimated from cyclic voltammetry (CV) in the range 0–1.0 V vs. SCE, using the total amount of charge by integrating the CV. After standing the electrode in the solution overnight, the electrode was conditioned by cycling 10 times at 5 mV $s^{-1}$ prior to the formal measurements. The potential scan rate, $v$, was 2–20 mV $s^{-1}$. Galvanostatic charge/discharge curves were also measured at 100–500 mA $g^{-1}$ for selected samples. Specific capacitance was calculated with respect to the total mass of composite, but if needed a net mass of $MnO_2$ in the electrode was used.

## 3 Results and discussion

### 3.1 Characterization of composites

The composite composition was estimated from the TG curve in oxygen as reported previously [19]. This method is sufficiently accurate, as confirmed from experimental results by dissolving $MnO_2 \cdot nH_2O$ in conc. HCl at 90 °C and weighing EG in the composite [19]. Possible contamination by potassium ions [10] was neglected here. The composition of the composites is shown in Table 1. The hydrated water number, $n$, is not the same but lies in an acceptable range.

XRD patterns of $MnO_2 \cdot nH_2O$-EG composites prepared with different amounts of EG, and $MnO_2 \cdot nH_2O$ prepared by method (1) without adding EG (referred to as 'pristine' $MnO_2 \cdot nH_2O$) are shown in Fig. 1. In addition to two sharp peaks assigned to EG, C 002 and C 004, weak and broad peaks are distinguished around $2\theta = 38^{\circ}$ and $67^{\circ}$. These are also observed for 'pristine' $MnO_2 \cdot nH_2O$ and can be reasonably assigned to $MnO_2 \cdot nH_2O$, but corresponding crystalline compounds were not found in the powder diffraction index. Apparently, no large differences were observed in XRD patterns for $MnO_2 \cdot nH_2O$ by different methods and for 'pristine' $MnO_2 \cdot nH_2O$.

Nitrogen adsorption/desorption isotherms for selected samples are shown in Fig. 2. The specific surface area of composites calculated from similar data is listed in Table 1. As the surface area of 'pristine' $MnO_2 \cdot nH_2O$

**Table 1** Parameters of prepared composites

| Sample code | Composition/mass% | | | Specific surface area/$m^2$ $g^{-1}$ |
|---|---|---|---|---|
| | EG | $MnO_2 \cdot nH_2O$ | ($n$) | |
| Method (1) | | | | |
| 1a | 2.3 | 97.7 | (0.83) | 258 |
| 1b | 12.9 | 87.1 | (0.66) | 255 |
| 1c | 23.9 | 76.1 | (0.65) | 237 |
| Method (2) | | | | |
| 2a | 8.7 | 91.3 | (0.71) | 229 |
| 2b | 17.3 | 82.7 | (0.59) | 219 |
| 2c | 33.9 | 66.1 | (0.81) | 213 |

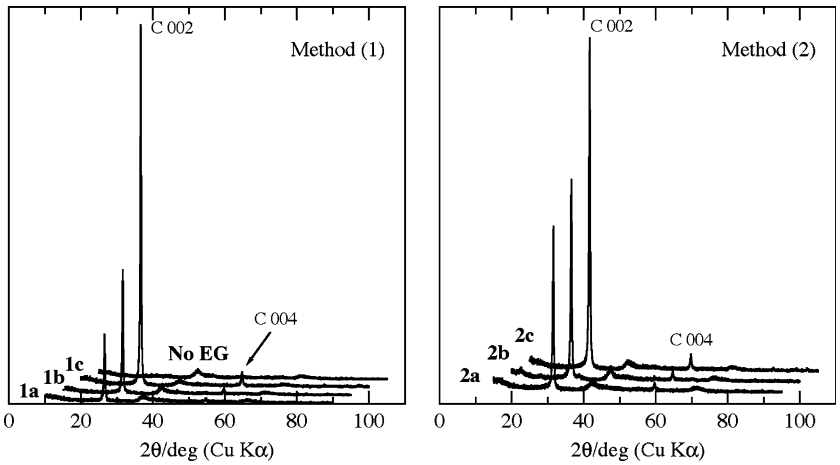


**Fig. 1** XRD patterns of the hydrated Mn(IV) oxide-EG composites. 'No EG' indicates $MnO_2 \cdot nH_2O$ prepared by method (1) without adding EG

was 293 $m^2\ g^{-1}$ and that of EG was about 60 $m^2\ g^{-1}$, most of the area is the contribution from the oxide. Generally, the surface area of the composites by Method (1) is larger than that by Method (2), independent of the amount of EG included. A significant feature of the isotherms due to the preparation method is distinguished clearly in Fig. 2. The isotherm for 'pristine' $MnO_2 \cdot nH_2O$ by Method (1) resembles Type IV, suggesting the presence of mesopores. The isotherm for **1b** is similar to 'pristine' $MnO_2 \cdot nH_2O$, whereas that for **2a** shows only small hysteresis and the shape is similar to Type II. Actually, computations of pore size distributions by the BJH method [21] revealed that peak pore volume was in a range 6–10 nm in diameter for 'pristine' $MnO_2 \cdot nH_2O$ and **1b** [19], but the pore volume for **2a** increased monotonically with decreasing pore size.

SEM photographs of **1c** and **2c** are shown in Fig. 3. It is evident that the preparation method significantly affects the morphology. In the case of Method (1) small $MnO_2 \cdot nH_2O$ particles are deposited sparsely on the graphite sheets of EG or dispersed separately (Fig. 3a, c), whereas Method (2) produces lumps of aggregated $MnO_2 \cdot nH_2O$ particles and, in some parts, pieces of EG are covered with a thick $MnO_2 \cdot nH_2O$ layer (Fig. 3b, d). The features of **2c** were similar for **2a** and **2b**, in which the EG content was lower. The difference may be because of the surface nature of EG and the formation scheme of $MnO_2 \cdot nH_2O$. The original EG is hydrophobic, but by Method (1) the EG surface is oxidized during the initial 1 h stirring in the $KMnO_4$ solution, which makes the surface hydrophilic as confirmed by separate experiments, and the procedure used is reported to form colloidal $MnO_2$ [20]. In contrast, by the procedure of Method (2) initially formed $MnO_2 \cdot nH_2O$ particles adsorb Mn(II) ions and grow by further reaction. The hydrophobic surface of EG may also promote the formation of large aggregates. Naturally, the sizes of primary particles formed by both methods are sub-micrometer or smaller as shown in Fig. 3c and d, which is reflected in the nitrogen adsorption behavior.

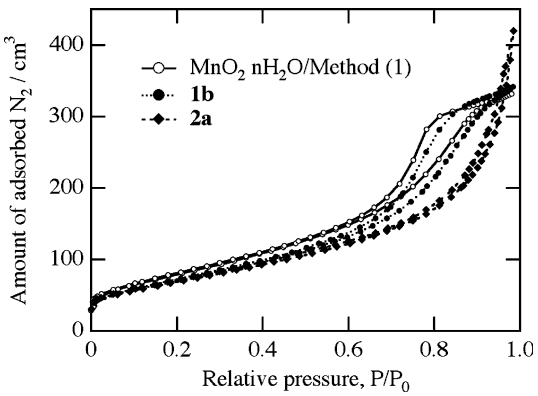


**Fig. 2** Nitrogen adsorption/desorption isotherms at 77 K for selected samples

### 3.2 Electrochemical properties of composites

CVs at 2 mV $s^{-1}$ in 1 mol $L^{-1}$ $Na_2SO_4$ electrolyte are shown in Fig. 4. As reported previously [19], the specific capacitance of 'pristine' $MnO_2 \cdot nH_2O$ is about 1 F $g^{-1}$, for poor electrical conductivity (normally order of 10 S $cm^{-1}$) as shown in Fig. 4a. The exfoliated graphite has a rectangular shape but also gives a very low capacitance, less than 2 F $g^{-1}$, as shown in Fig. 4b, and the capacitive contribution by EG to the composites is negligible. The potential jumps at the lower and higher ends become steeper, that is, the rectangular characteristics of the CV are nearly achieved, with increasing amounts of EG. However, the amount of EG to attain good capacitive characteristics is smaller by Method (1) than by Method (2). In addition, the total capacitance per composite, which is proportional to the area of the CV, is larger by Method (1) than Method (2) as shown in Fig. 5a by the open symbols. The total capacitance does not change much with increasing amount

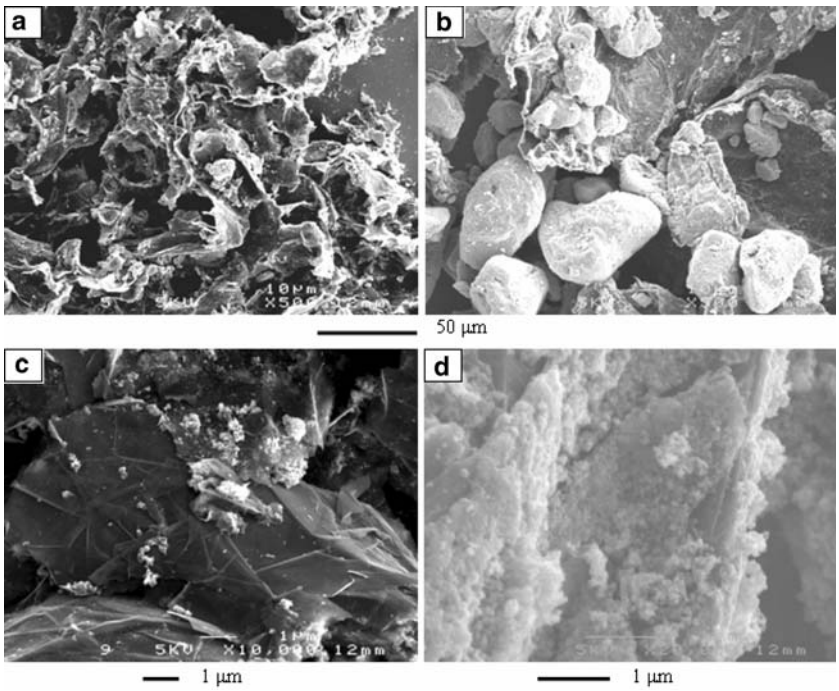


**Fig. 3** SEM photographs of (**a**, **c**) **1c** and (**b**, **d**) **2c** (cf. Table 1) at different magnifications

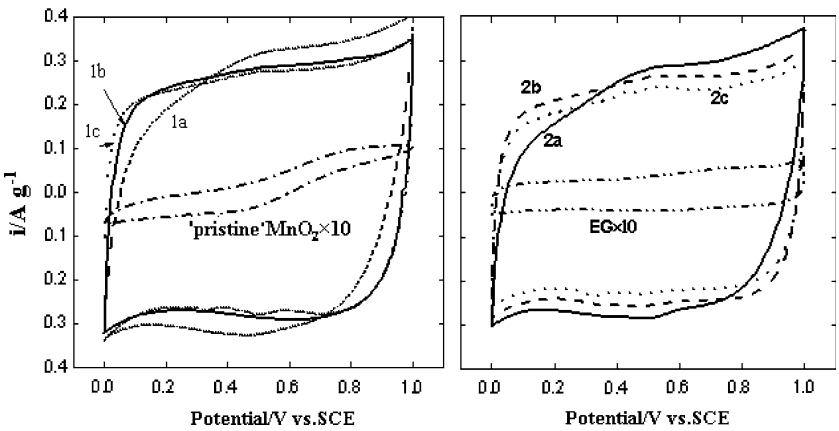


**Fig. 4** Cyclic voltammograms at 2 mV $s^{-1}$ in 1 mol $L^{-1}$ · $Na_2SO_4$ electrolyte

of EG, but the capacitance per net amount of $MnO_2$ is almost proportional to the EG content, as indicated by the filled symbols. Similarly to the report using carbon black [15], the utilization ratio of $MnO_2$ increases with EG content and the effect is more prominent in the case of Method (1). Increase in EG content, however, decreases the amount of active mass in the electrode so that there is a limit, as seen in the change from **2a** to **2c** in Fig. 5a. These results can be reasonably ascribed to the morphology (Fig. 3), which produces a better electrical contact of the composites and mesopores by Method (1) (Fig. 2). As shown in Fig. 5b, the total capacitance decreases slightly with increasing surface area, except for **2c**, which contains large amounts of EG. Decrease in capacitance per net amount of $MnO_2$ is much more marked, as shown by the filled symbols. As the greater part of the surface area originates from $MnO_2 \cdot nH_2O$, the results in Fig. 5b suggest that the contribution from the electrical double layer is minimal. It is deduced from the nitrogen adsorption/desorption isotherms (Fig. 2) that the difference in the pore structure may have a more significant effect on the capacitance, if anything. It has been reported by several authors that increased specific surface area of $MnO_2 \cdot n$-$H_2O$ does not contribute proportionally to the capacitance [7, 22].

CVs at different scan rates for **1c** and **2b** are shown in Fig. 6. Although the potential jump at the lower and higher ends delays and the capacitance decreases with increasing scan rate, again the rectangular characteristics are better for **1c** than **2b**. Distortion of the CV and decreased capacitance are mainly due to the increase in the inaccessible sites within the composite electrode at higher

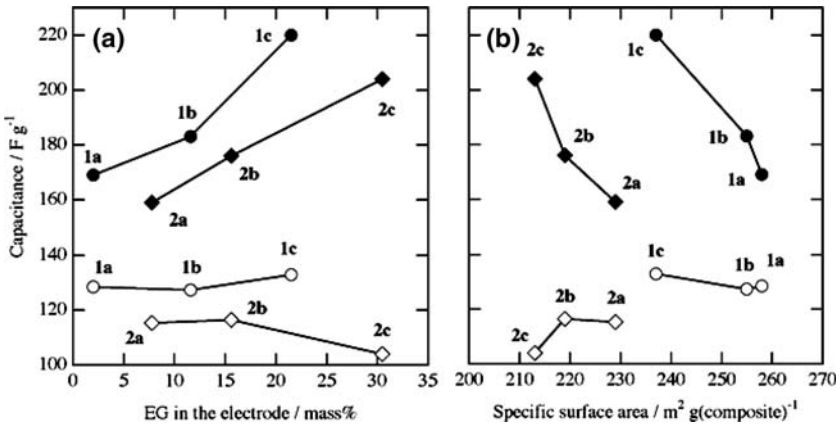


**Fig. 5** Summaries of the total capacitance calculated from cyclic voltammograms at 2 mV $s^{-1}$ in 1 mol $L^{-1}$ $Na_2SO_4$ solution. Open symbols are calculated per amounts of composite in the electrode and filled ones per net amounts of $MnO_2$

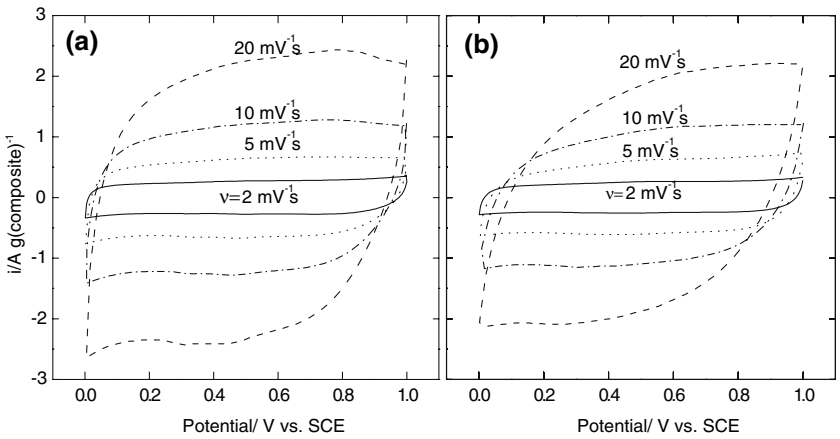


**Fig. 6** Cyclic voltammograms at different scan rates for (**a**) **1c** and (**b**) **2b** (cf. Table 1)

scan rates; that is, a delay of transport within the composites rather than the slow redox reactions of active materials. It has been reported that there is a relationship between voltammetric charge, $q$, and scan rate, $v$, which was observed with conducting oxide electrocatalysts prepared by thermal decomposition [23, 24]. Supposing the reversible redox transition by mobile ions, probably protons and possibly sodium ions in the present case, the extrapolation of $q$ to $v = \infty$ from the $q$ vs. $v^{-1/2}$ plot gives the outer charge, $q_O$, which is the charge resulting from the most accessible surface sites, whereas the extrapolation of $q$ to $v = 0$ from the $q$ vs. $v^{1/2}$ plot gives the charge from accessible total sites, $q_T$ [8]. The results for **1c** and **2b** are shown in Fig. 7. The $q$ vs. $v^{-1/2}$ plots are not linear but here $q_O$ was estimated by the least squares method as shown in Fig. 7b. The estimated charges were $q_T = 232$ F $g^{-1}$ and $q_O = 138$ F $g^{-1}$ for **1c**, and $q_T = 206$ F $g^{-1}$ and $q_O = 90$ F $g^{-1}$ for **2b**. The lower ratio of $q_O/q_T$ for **2b** indicates that there are larger amounts of the inner and less accessible sites in the composite by Method (2) than Method (1). This result is consistent with the morphology of the composites and also with the pore size distribution (cf. difference in the adsorption isotherms in Fig. 2).

Figure 8 shows the charge/discharge behavior of **1c** and 2**b** in the potential range 0–1.0 V vs. SCE at different current densities in a 1 mol $L^{-1}$ $Na_2SO_4$ solution. The curves are approximately symmetrical and linear for both charge and discharge portions, except for small *ir* drops of less than 5 Ω at all current densities. Curves for both samples show a similar shape, but the capacitances of 2**b** are smaller. The averages of charge/discharge capacitances at 100 and 200 mA $g^{-1}$ were 124 F g(composite)$^{-1}$ (205 F g-$(MnO_2)^{-1}$) for **1c** and 108 F g(composite)$^{-1}$ (163 F g$(MnO_2)^{-1}$) for **2b**. The reported values of specific capacitance for hydrated manganese(IV) oxide are in a range between 130 and 250 F $g^{-1}$ [3–14], though they cannot be compared simply due to different measuring methods and basis of capacitance calculation. The above results indicate that EG is a good conductive material for $MnO_2 \cdot nH_2O$ electrochemical capacitors if appropriate synthesis processes are used.

## 4 Conclusion

Two different routes were used to synthesis the $MnO_2 \cdot nH_2O$–EG composites for electrochemical capaci-

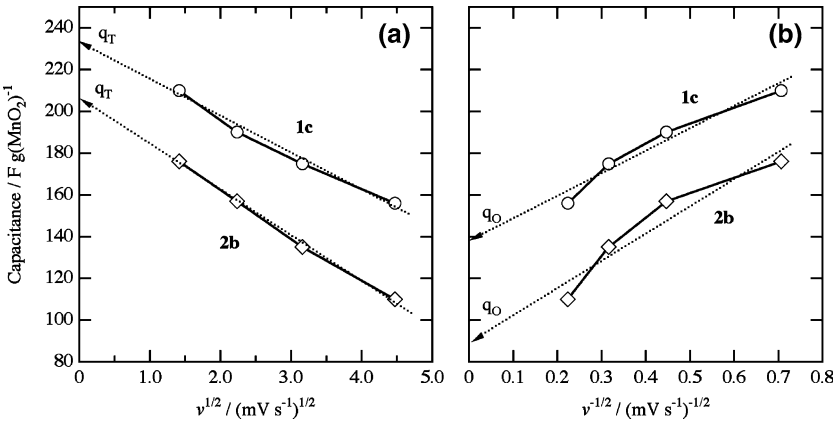


**Fig. 7** Dependence of the capacitance of (**a**) **1c** and (**b**) **2b** (cf. Table 1) on the potential scan rate

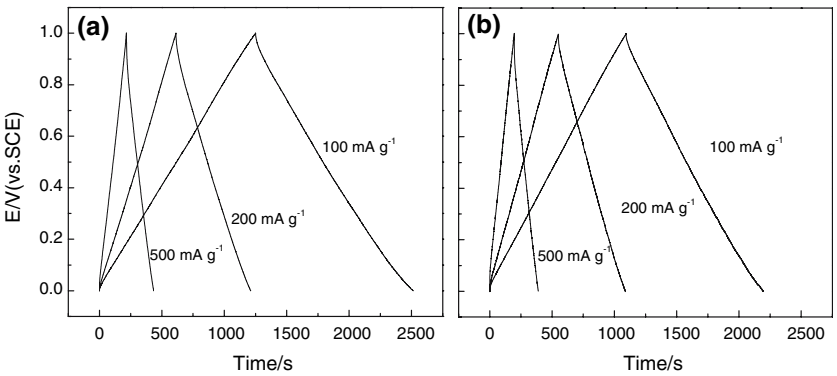


**Fig. 8** Galvanostatic charge/discharge behavior of (**a**) **1c** and (**b**) **2b** (cf. Table 1)

tors using potassium permanganate and manganese(II) acetate solutions as starting materials and commercially available low cost EG as a conductive substrate. The physical and electrochemical capacitor properties of the products were measured using XRD, nitrogen adsorption/desorption, SEM, thermogravimetric analysis, cyclic voltammetry and galvanostatic charge/discharge measurement. The results of Nitrogen adsorption/desorption isotherms and SEM showed that submicrometer or smaller sized $MnO_2 \cdot nH_2O$ particles having mesopores were obtained by Method (1) while lumps of aggregated particles of several tens of micrometers without mesopores were formed by Method (2). Electrochemical measurements revealed that the amount of EG to attain good capacitive characteristics is smaller by Method (1) than Method (2). The capacitance per net amount of $MnO_2$ in 1 mol $L^{-1}$ $Na_2SO_4$ solution obtained from CV measurements increased proportionally with EG content and was always larger by Method (1) than Method (2). Meanwhile, the utilization ratio of $MnO_2$ increased with EG content and the effect was more prominent in the case of Method (1). The results revealed that the performance of the composite strongly depends on synthesis method, even from the same starting materials and EG can be used as a good conductive material for $MnO_2 \cdot nH_2O$ electrochemical capacitors and $MnO_2 \cdot nH_2O$/EG composite having a good capacitive characteristics can be obtained if appropriate synthesis processes are used. Compared to their composition, the morphology of the products was a primary factor leading to different electrochemical performance.

**Acknowledgements** A part of the present work was supported by a Grant-in-Aid for Scientific Research (B) from JSPS (No. 18350102) and by Shanghai Leading Academic Discipline Project (No. P1501)

## References

1. Conway BE (1991) J Electrochem Soc 138(6):1539
2. Sarangapani S, Tilak BV, Chen CP (1996) J Electrochem Soc 143(11):3791
3. Lee HY, Goodenough JB (1999) J Solid State Chem 144(1):220
4. Pang SC, Anderson MA, Chapman TW (2000) J Electrochem Soc 147(2):444
5. Lee HY, Kim SW, Lee HY (2001) Electrochem Solid-State Lett 4(3):A19
6. Hu CC, Tsou TW (2002) Electrochem Comm 4(2):105
7. Jeong YU, Manthiram A (2002) J Electrochem Soc 149(11):A1419
8. Jiang J, Kucernak A (2002) Electrochim Acta 47(15):2381
9. Hu CC, Tsou TW (2002) Electrochim Acta 47(21):3523
10. Toupin M, Brousse T, Bélanger D (2002) Chem Mater 14(9):3946
11. Hu CC, Tsou TW (2003) J Power Sources 115(1):179
12. Reddy RN, Reddy RG (2003) J Power Source 124(1):330
13. Jones DJ, Wortham E, Roziére J, Favier F, Pascal JL, Monconduit L (2004) J Phys Chem Solids 65(2–3):235

14. Wu MS, Chiang PCJ (2004) Electrochem Solid-State Lett 7(6):A123
15. Chang JK, Lin CT, Tsai WT (2004) Electrochem Commun 6(7):666
16. Raymundo-Piñero E, Khomenko V, Frackowiak E, Beguin F (2005) J Electrochem Soc 152(1):A229
17. Wang GX, Zhang BL, Yu ZL, Qu MZ (2005) Solid State Ionics 176(11–12):1169
18. Lee CY, Tsai HM, Chuang HJ, Li SY,Lin P, Tseng TY (2005) J Electrochem Soc 152(4):A716
19. Wan CY, Azumi K, Konno H (2007) Electrochim Acta 52(9):3061
20. Morgan JJ, Stumm W (1964) J Colloid Sci 19:347
21. Barrett EP, Joyner LG, Halenda PP (1951) J Am Chem Soc 73:373
22. Kim H, Popov BN (2003) J Electrochem Soc 150(3):D56
23. Ardizzone S, Fregonara G, Trasatti S (1990) Electrochim Acta 35(1):263
24. DePauli CP, Trasatti S (1995) J Electroanal Chem 396(1–2):161